

THE FLORIDA STATE UNIVERSITY
COLLEGE OF ARTS AND SCIENCES

A CHEMICAL AND METEOROLOGICAL ANALYSIS OF
LONG-RANGE TRANSPORT FROM AFRICA
DURING AUSTRAL SPRING

By

DANIELLE M. MORSE

A Thesis submitted to the
Department of Meteorology
in partial fulfillment of the
requirements for the degree of
Master of Science

Degree Awarded:
Summer Semester, 2005

The members of the Committee approve the thesis of Danielle M. Morse defended on July 13, 2005.

Henry E. Fuelberg
Professor Directing Thesis

Jon Ahlquist
Committee Member

Philip Cunningham
Committee Member

The Office of Graduate Studies has verified and approved the above named committee members.

ACKNOWLEDGMENTS

I would like to thank my major professor, Dr. Henry Fuelberg, for all his support and help throughout my stay at FSU. I would also like to thank the members of my committee, Dr. Jon Ahlquist and Dr. Philip Cunningham. Thanks go as well to all the Fuelberg Lab, especially Chris Kiley and Mike Porter.

This research was funded by NASA grant NNG04GC33G under the Tropospheric Chemistry program. I would like to thank Dr. James Crawford from NASA and Dr. Nicola Blake from UCI-Irving who have been invaluable aides in the chemical analysis.

TABLE OF CONTENTS

List of Tables	v
List of Figures	vi
Abbreviations and Acronyms	viii
Abstract	ix
Chapter 1. INTRODUCTION.....	1
Chapter 2. DATA AND METHODOLOGY	5
2.1 Meteorological Data.....	5
2.2 Chemical Data.....	6
Chapter 3. RESULTS.....	9
3.1 Transport from Africa.....	9
3.2 Chemical Evolution during Transport	16
Chapter 4. SUMMARY AND CONCLUSIONS.....	34
REFERENCES	38
BIOGRAPHICAL SKETCH	42

LIST OF TABLES

1. Lifetimes of chemical tracers used in this study. Upper troposphere is above 350 hPa, or 8 km. Mid-troposphere is 600 hPa to 350 hPa, or 4-8 km.....	8
2. Mean values for species from groupings discussed in Figures 9 through 14.	22
3. Physical mixing lifetime calculated from equation (2) for the four species used in this study.	33

LIST OF FIGURES

<p>1. Mean streamlines and isotachs during PEM-Tropics A period for a) 300 hPa and mean streamlines for b) 500 hPa and c) 1000 hPa. The shaded areas are winds greater than 30 m s^{-1} with an isotach interval of 10 m s^{-1}.....</p>	3
<p>2. Along Track Scanning Radiometer (ATSR) global fire map for a) August 1996 and b) September 1996. Grey dots indicate fire locations. Data were available from http://dup.esrin.esa.it/.....</p>	10
<p>3. Ten-day forward trajectories initialized at 10°E and 50°E between 350 hPa and 200 hPa throughout the month of September 1996. The trajectories are separated into 5 transport categories: a) zonal, b) Australian anticyclonic, c) western Pacific anticyclonic, d) Easter Island anticyclonic, and e) South American anticyclonic. Between 100 and 200 representative trajectories are shown from each category. Circles indicate starting points; x's indicate ending points. The upper panel is a plan view; the lower is longitude vs. altitude (hPa).....</p>	12
<p>4. Ten-day forward trajectories as in Figure 3, but with starting altitudes between 600 hPa and 300 hPa. The three transport categories shown are: a) zonal, b) Australian anticyclonic, and c) western Pacific anticyclonic.</p>	13
<p>5. Ten-day forward trajectories initialized at 180° between 15°S and 40°S and 500 hPa and 200 hPa. Fifty sample trajectories from the two categories are shown: a) Easter Island anticyclonic and b) South American anticyclonic.....</p>	15
<p>6. Ten day backward trajectories from PEM-Tropics A upper tropospheric flight paths (above 350 hPa) that extend back to Africa. Trajectories are grouped by the time required to reach Africa: a) 4 days, b) 5 days, c) 6 days, d) 7 days and e) 8 days</p>	18
<p>7. Ten day backward trajectories from PEM-Tropics A mid tropospheric flight paths (600 hPa to 350 hPa) that extend back to Africa. Trajectories are grouped by time required to reach Africa: a) 5 days, b) 6 days, c) 7 days, d) 8 days and e) 9 days</p>	19

8. Locations of points along flight tracks during PEM-Tropics A from which backward trajectories reach Africa during various time intervals (color bar) for a) upper tropospheric and b) mid tropospheric flight segments ..	21
9. Correlation plot of ethane versus propane for high altitudes (above 350 hPa) for all TRACE-A data and PEM-Tropics A data corresponding to trajectories in Figure 6. The upper panel shows all values; the * is values collected during TRACE-A at low altitudes near a biomass burning source [from <i>Mauzerall et al.</i> , 1998]. The solid line is the expected relationship based only physical mixing of inert species; the dashed-dotted line is the relationship based only on OH scavenging. The dashed line is the regression fit through all data points. The intersection of the lines is along the regression line at the greatest observed value of propane. The lower panel shows mean values for PEM-Tropics A 2 day groupings and the TRACE-A data set as well as the lines from the upper panel	24
10. As in Figure 9, but a correlation plot of ethane versus propane for mid tropospheric collection levels, 600 hPa to 350 hPa. The lines and points have the same meaning as in Figure 9	25
11. As in Figure 9, but a correlation plot of CO versus ethyne for upper tropospheric levels. The lines and points have the same meaning as in Figure 9.....	27
12. As in Figure 9, but a correlation plot of CO versus ethyne for mid tropospheric levels. The lines and points have the same meaning as in Figure 9.....	28
13. As in Figure 9, but a correlation plot of ethane versus ethyne for upper tropospheric levels. The lines and points have the same meaning as in Figure 9.....	29
14. As in Figure 9, but a correlation plot of ethane versus ethyne for mid tropospheric levels. The lines and points have the same meaning as in Figure 9.....	30
15. Ten-day backward and ten-day forward trajectories from the sampling locations in Figure 6, upper troposphere (a) and Figure 7, mid troposphere (b). Only approximately 100 representative trajectories are shown.	37

ABBREVIATIONS AND ACRONYMS

ATSR	Along Track Scanning Radiometer
CDF	cumulative distribution function
CO	carbon monoxide
ECMWF	European Centre for Medium-Range Weather Forecasts
GTE	Global Tropospheric Experiment
hPa	hectopascal
ITCZ	Intertropical Convergence Zone
km	kilometer
$m s^{-1}$	meters per second
min	minute
NASA	National Aeronautics and Space Administration
NMHC	non-methane hydrocarbon
PEM	Pacific Exploratory Mission
ppbv	parts per billion by volume
pptv	parts per trillion by volume
TRACE-A	Transport and Atmospheric Chemistry near the Equator- Atlantic
UTC	Universal Time Coordinated

ABSTRACT

During the austral spring months of September and October when biomass burning is prevalent in the Southern Hemisphere, long-range transport can move the biomass burning byproducts from southern Africa to the Pacific Basin. Meteorological data from September 1996 were used to examine the transport from Africa using forward trajectories. Long-range transport is defined as trajectories that extend from Africa eastward to at least 110°E within 10 days. Five categories were found from trajectory analysis to constitute the major long-range transport pathways: zonal flow (35%) and four anticyclonic flows over Australia (5%), the western Pacific (5%), Easter Island (0.8%) and South America (0.9%). Chemical data collected during NASA's Pacific Exploratory Mission-Tropics, Phase A (PEM-Tropics A) and Transport and Atmospheric Chemistry near the Equator- Atlantic (TRACE-A) missions were studied to determine the chemical evolution of burning byproducts during the long-range transport. Photochemical decay and physical mixing with background air were both found to be important dilution processes, with estimates of physical mixing lifetimes shorter than photochemical decay lifetimes. Greater values of pollution were detected at mid-tropospheric altitudes over the Pacific Basin, suggesting that more pollution is transported to mid-levels at long ranges.

CHAPTER 1

INTRODUCTION

The remote South Pacific Basin was long considered an area of the world with the least anthropogenic influence on air quality. However, NASA's Pacific Exploratory Mission-Tropics, Phase A (PEM-Tropics A), conducted during the austral spring months of August to October 1996, discovered widespread biomass burning influences over the Pacific [Hoell *et al.*, 1999]. Biomass burning was prevalent in the African subcontinent, South America, and Australia during the 1996 season [Olson *et al.*, 1999] and during an earlier NASA mission, TRansport and Atmospheric Chemistry near the Equator-Atlantic (TRACE-A, September to October 1992) [Fishman *et al.*, 1996]. Long-range transport advects the pollution created by these fires around the world, including to the South Pacific Basin [e.g., Fuelberg *et al.*, 1999].

Greater than expected values of biomass burning indicator species were found over the Pacific during the PEM-Tropics A period. Analyses of carbon dioxide, ozone, acidic species, non-methane hydrocarbons (NMHC's) and halocarbons indicated the residuals of biomass burning from upstream sources [Vay *et al.*, 1999; Schultz *et al.*, 1999; Talbot *et al.*, 1999; Blake *et al.*, 1999]. Dibb *et al.* [1999] used the radioactive tracer Pb-210 to derive transit times between 5-14 days for most plumes over the Pacific. Since NMHC's are depleted photochemically in the atmosphere at specific rates, ratios of species that deplete at different rates have been used to estimate the ages of plumes [Mauzerall *et al.*, 1998]. Conversely, relatively fresh plumes (less than 1 week) were sampled during the TRACE-A campaign [Mauzerall *et al.*, 1998, Gregory *et al.*, 1996], while older plumes were sampled during the PEM-Tropics B campaign (February to April, 1999) [Martin *et al.*, 2002]. McKeen *et al.* [1993, 1996], who examined hydrocarbon ratios for low altitude parcels during the PEM-West A campaign (September to October 1991), determined that physical mixing was more important to depletion than photochemical loss.

Mean meteorological conditions calculated from ECMWF model data during PEM-Tropics A (Figure 1) explain transport patterns over the South Pacific Basin. The 1000 hPa chart (Figure 1c) shows several quasi-permanent features during austral spring. The Intertropical Convergence Zone (ITCZ) is strong and prevalent near 10°N. Flow over the Pacific Ocean is mostly from the west poleward of 30°S and from the east in the tropics. A semi-permanent anticyclone is located near Easter Island in the eastern Pacific, while indications of weaker transient cyclones and anticyclones are visible along the mid-latitude storm track. Low level flow over the Indian Ocean is more complex, with zonal flow at high latitudes and meridional flow near the equator associated with the Indian monsoon. At higher altitudes, the anticyclones are shifted northward and are weaker. Streamlines at 500 hPa (Figure 1b) show an anticyclone over the eastern Pacific near 20°S, and several weak anticyclones over the Indian Ocean near the equator. Strong zonal flow is evident at 500 hPa in the higher latitudes. The 300 hPa plot (Figure 1a), with isotachs shaded for winds stronger than 30 m s⁻¹, shows the location of the upper-level jet stream. The strongest speeds of 50 m s⁻¹ are southwest of Australia. This zonal flow at both the middle and upper levels is the primary transport mechanism from Africa and South America to the Pacific. In the eastern Pacific, a secondary upper-level flow regime is westward from South and Central America in the weaker easterly flows [Fuelberg *et al.*, 1999; Blake *et al.*, 1999]. Additional information about the mean circulation of the Southern Hemisphere can be found in Hurrell *et al.* [1998] and Newell *et al.* [1972].

Several studies have shown that numerical models can simulate the transport of pollution from Africa to the Pacific. Specifically, burning byproducts first are pumped from the surface to higher altitudes by convection [Fuelberg *et al.*, 1999; Dibb *et al.*, 1999; Pickering *et al.*, 1996] or by middle latitude cyclones and fronts [Bethan *et al.*, 1998]. The polluted air then can either be immediately advected eastward by the strong upper-level zonal flow [Staudt *et al.*, 2002; Singh *et al.*, 2000] or can circulate in an anticyclone over the South Atlantic Ocean [Chatfield *et al.*, 1998]. This Atlantic plume later is “gated” by frontal systems into the same strong zonal flow, arriving in plumes over the Pacific [Chatfield *et al.*, 2002]. Forward trajectories from Africa and South

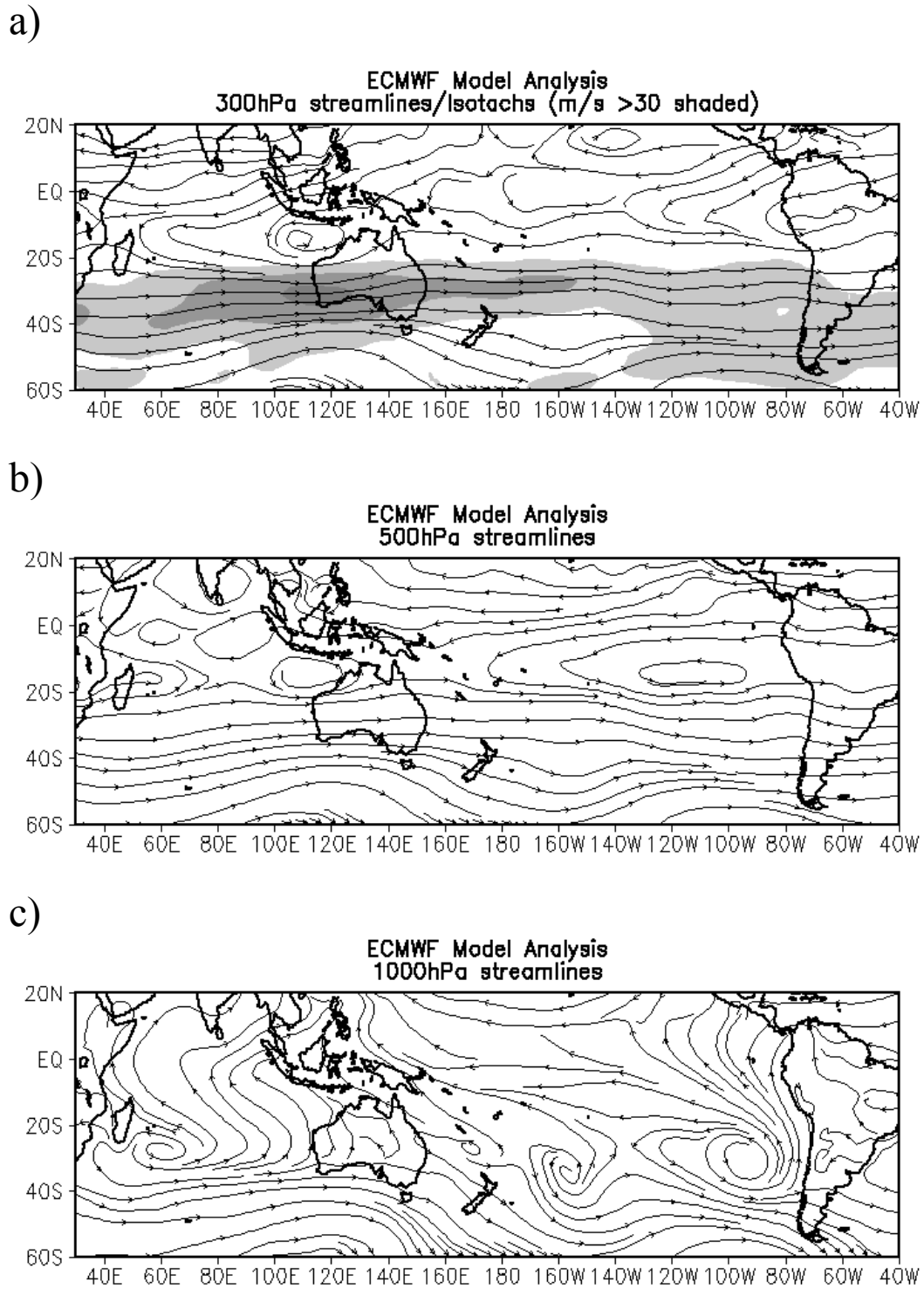


Figure 1. Mean streamlines and isotachs during PEM-Tropics A period for a) 300 hPa and mean streamlines for b) 500 hPa and c) 1000 hPa. The shaded areas are winds greater than 30 m s^{-1} with an isotach interval of 10 m s^{-1} .

America also have shown transport from Africa into the Pacific Basin [*Lusher*, unpublished manuscript, 1999]. Backward trajectories from plumes that were detected during PEM-Tropics A showed source regions in South America and Africa, as well as southern Asia and the Northern Hemisphere [*Dibb et al.*, 1999; *Board et al.*, 1999; *Blake et al.*, 1999; *Fenn et al.*, 1999].

Using back trajectories and NMHC data from PEM-Tropics A, this paper describes the major pathways by which biomass burning byproducts are transported from Africa to the Pacific Basin, where this pollution dissipates over the Pacific Ocean in several sink areas. Sink areas will be shown to include the tropics, subsidence around the semi-permanent high pressure near Easter Island, and flow around storm systems that move across the mid-latitudes and over South America. Transport levels and times from Africa to the PEM-Tropics A aircraft will be investigated. This paper also examines the relative amounts of photochemical depletion and physical mixing that pollution experiences during the transport, along with estimates of mixing lifetime. The preferred level of injection and transport of the burning byproducts also will be discussed.

CHAPTER 2

DATA AND METHODOLOGY

2.1 Meteorological Data

We used meteorological data from the European Centre for Medium-Range Weather Forecasts (ECMWF) to determine transport pathways during the PEM-Tropics A mission. The gridded global data were at $2.5^\circ \times 2.5^\circ$ horizontal resolution, with 15 constant pressure levels, and available at 0000 and 1200 UTC. We used the lowest 13 pressure levels between 1000 hPa and 50 hPa.

Backward and forward kinematic trajectories were calculated using the three dimensional wind components. The scheme uses cubic spline interpolation to obtain data at 5 hPa vertical increments. The data also were interpolated to 5 min time intervals. Details of the trajectory model are found in *Fuelberg et al.* [1996, 1999, 2000] and *Martin et al.* [2002]. Compared to earlier versions of the model, the current trajectories were not terminated if they intersected the lower boundary, but instead continued isobarically along the boundary and possibly were lofted by vertical motion at a later time, a procedure similar to *Stohl et al.* [1995]. Another important difference is that the current advection scheme now is iterative over a 5 min interval, creating more precise trajectories.

Trajectories were begun from two types of initial locations. NASA used two aircraft, a DC-8 and a P-3B, to collect chemical data over the Pacific during PEM-Tropics A. Ten-day backward and forward trajectories were calculated at 5 min intervals along the two sets of flight tracks. A 15 point diamond-shaped cluster of trajectories centered on the original flight track points at 5 min intervals was calculated to help reveal trajectory uncertainties due to wind shear. The points of this diamond were spaced 2.5° from the center point (5 points), with the pattern repeated 25 hPa above and below the flight level (an additional 10 points). The ECMWF data were interpolated temporally such that each cluster was initialized at the appropriate 5 min interval.

The second set of trajectories began at a group of “walls” from which 10-day forward trajectories were calculated each day during September 1996, initialized at 0000 UTC. Each wall consisted of 272 points, spaced along a longitude line at a 2.5° latitude interval between the equator and 40° S, with vertical locations every 50 hPa from 950 hPa to 200 hPa, inclusive. These walls were placed along several longitude bands including 10° E, 50° E and 180°.

There are several sources of uncertainty in trajectory calculations. These include the spatial and temporal resolution of the ECMWF data, errors in the location or intensity of meteorological features in the ECMWF analysis, and errors in the numerical calculations. Studies that address these limitations include *Stohl et al.* [1995] and *Stohl and Seibert* [1998]. The Pacific Basin is a relatively data sparse area, so meteorological features there often are depicted less accurately than in more data-dense regions. Since deep convection and other mesoscale processes are not accurately resolved, trajectories do not represent these processes well. Trajectories also become less reliable over longer time periods. Nonetheless, trajectories calculated using the kinematic method have been widely used [e.g., *Martin et al.*, 2002; *Fuelberg et al.*, 1999, 2000; *Maloney et al.* 2001; *Stohl et al.*, 1999; *Hannan et al.*, 2003; *Swap et al.*, 1996, *Gregory et al.*, 1996].

2.2 Chemical Data

A set of in situ aircraft-derived chemical data was collected during PEM-Tropics A and TRACE-A by different investigators. The chemicals were sampled at various frequencies depending on the instrument. *Hoell et al.* [1999] described the species detected, the instruments, sampling techniques and intervals, as well as the limits of detection for the instruments of PEM-Tropics A. *Fishman et al.* [1996] gave a similar description for the TRACE-A mission. Merged data sets for both missions are available at the NASA-GTE ftp site (TRACE-A:

<ftp://ftp-gte.larc.nasa.gov/pub/TRACEA/MERGES/hydro/>; PEM-Tropics A:

<ftp://ftp-gte.larc.nasa.gov/pub/PEMTROPICSA/MERGES.V31/>). The merges contain flight and chemical information at various common time intervals. Since most of the species that we examined were collected in whole air samples at intervals of approximately 3 min, a data merge based on these samples was used. Thus, the values of

the species collected at greater frequencies were averaged during the whole air sampling period of approximately 1 min.

Various chemical species have been used in previous studies to infer the age and history of air samples [e.g., *Mauzerall et al.*, 1998; *Blake et al.*, 1999; *Martin et al.*, 2002]. The sources and lifetimes of species used in this study are described below. Photochemical lifetimes can vary based on pressure, temperature and humidity. We used two different altitude ranges in the troposphere, upper and middle, with corresponding photochemical lifetimes given in Table 1 [Dr. James Crawford, personal communication]. The upper troposphere is defined to be above 350 hPa, or approximately 8 km, while the mid-troposphere is between 600 hPa and 350 hPa, or approximately 4 to 8 km.

There are many sources of carbon monoxide (CO), a byproduct of combustion such as biomass burning and urban fossil fuel consumption [*Blake et al.*, 1999]. CO has a pressure dependent photochemical lifetime of several months in the troposphere. Ethyne (C₂H₂) is a non-methane hydrocarbon emitted from incomplete combustion that has sources similar to those of CO [Dr. Nicola Blake, *personal communication*], but with a shorter lifetime. Propane (C₃H₈) and ethane (C₂H₆) are NMHCs with similar sources emitted from the combustion of both fossil fuels and biomass [*Hao et al.*, 1996]. Ethane has the longest lifetime of the species we examine, while propane has the shortest.

Background mixing ratios for most species are different in stratospheric air. Samples at high altitudes with values of ozone (O₃) exceeding 125 parts per billion by volume (ppbv) were removed from the data set. Thus, our study considers only the troposphere.

Table 1. Lifetimes of chemical tracers used in this study. Upper troposphere is above 350 hPa, or 8 km. Mid-troposphere is 600 hPa to 350 hPa, or 4-8 km.

<i>Species</i>	<i>Upper Troposphere</i>	<i>Mid- Troposphere</i>
Carbon Monoxide (CO)	66 days	61 days
Ethyne (C ₂ H ₂)	26 days	21 days
Propane (C ₃ H ₈)	20 days	15 days
Ethane (C ₂ H ₆)	132 days	84 days

CHAPTER 3

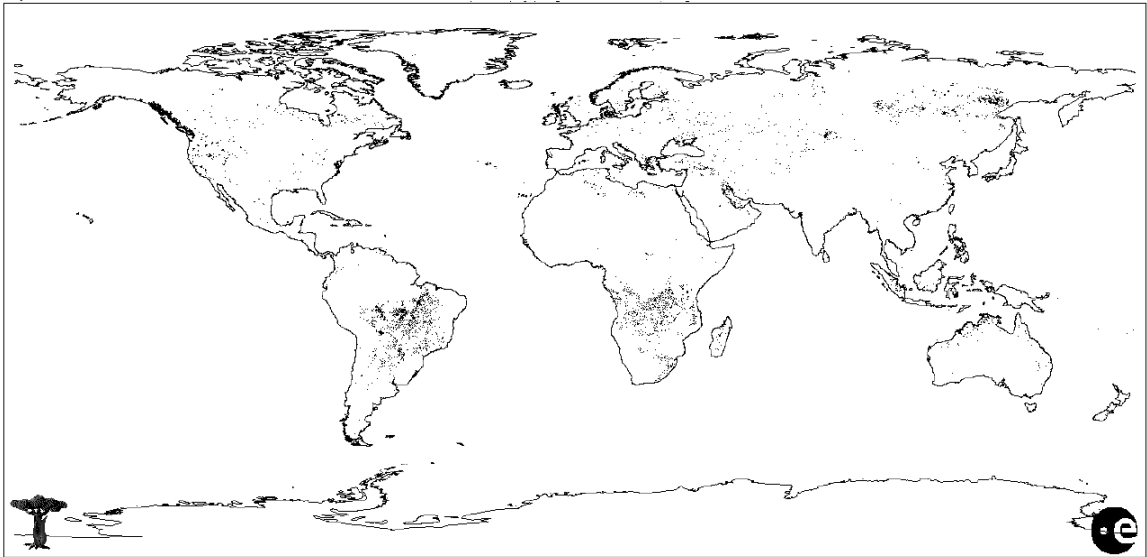
RESULTS

Several areas contained extensive biomass burning during the austral spring of 1996, including South America, southern Africa and Australia [Olson *et al.*, 1999]. Global fire data from the Along Track Scanning Radiometer (ATSR) during August and September 1996 (Figure 2) show that the fires in Africa and South America are widespread throughout the PEM-Tropics A period; however, there are fewer fires in Australia, and they occur mostly during September. Byproducts from these fires can be carried off the African continent to both the east and west, depending on local meteorological conditions. Garstang *et al.* [1996] demonstrated that between August and October 1992 (the TRACE-A year) over 75% of forward trajectories from Africa eventually were transported eastward towards the Indian Ocean Basin across the 40°E longitude line, sometimes after circulating in an anticyclone over the African continent for several days. We will use meteorological data from 1996 to examine this transport on a long-range scale.

3.1 Transport from Africa

Ten-day forward trajectories were initialized along two “walls” of longitude, 10°E and 50°E, thereby bracketing the continent of Africa. The trajectories were started at 0000 UTC every day during September 1996, yielding a total of 9180 trajectories. The trajectories that reached at least 110°E (43% of the total) were considered long-range and were sorted into five categories depending on their path and destination. The five categories are zonal flow and four longitude bands containing anticyclonic transport: Australia, 110°E to 150°E; western Pacific, 150°E to 120°W; Easter Island, 120°W to 80°W; and South America, 80°W to 40°W. These categories are not exclusive; thus, a trajectory could be counted in more than one category. The possible overlap between

a)



b)

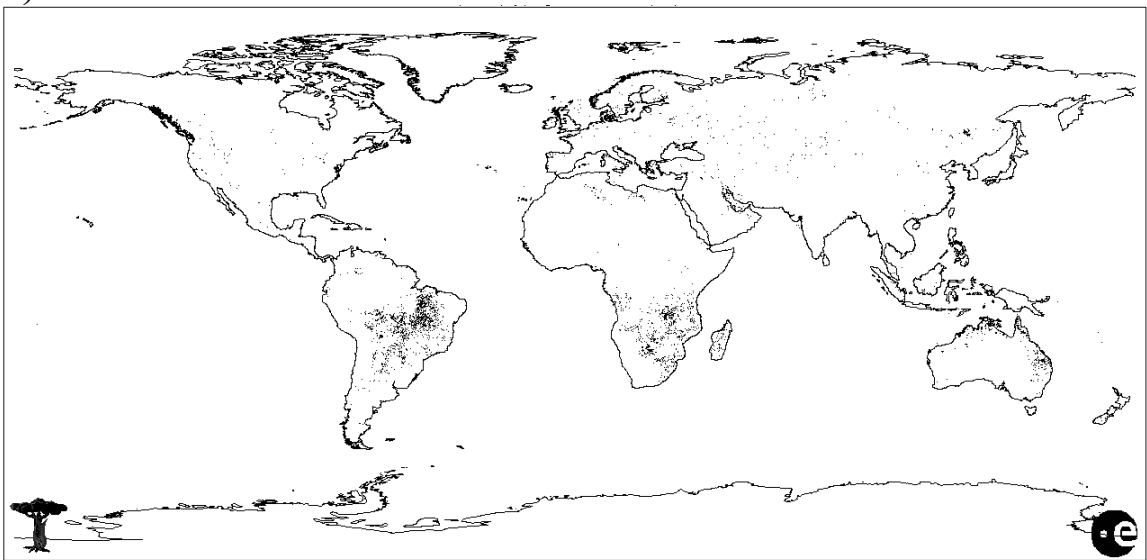


Figure 2. Along Track Scanning Radiometer (ATSR) global fire map for a) August 1996 and b) September 1996. Grey dots indicate fire locations. Data were available from <http://dup.esrin.esa.it/>

categories is necessary since any scheme to count a trajectory in only one category would require ranking the relative importance of the categories.

Figures 3 and 4 show representative trajectories for the five categories. For clarity of presentation, the total trajectories in each category are represented by between 100 and 200 trajectories throughout the 30-day period. The starting altitudes are separated into two groups, upper troposphere (350 hPa to 200 hPa, Figure 3) and mid troposphere (600 hPa to 350 hPa, Figure 4). The prime meridian is the cutoff for plotting purposes.

The zonal flow category (Figures 3a and 4a) accounts for 81% of the long-range trajectories (35% of the total). The high altitude zonal transport (Figure 3a) mostly is due to the jet stream, which has average speeds exceeding 30 m s^{-1} during the period (Figure 1a). However, wind speeds vary greatly from day to day and with location, causing some trajectories to barely reach the Pacific Basin within the 10 day period, while others nearly circle the globe during that time. The zonal transport mostly is confined to the latitude band 20°S to 60°S over the Pacific Basin, with a few exceptions farther south and north. The mid-level zonal transport (Figure 4a) generally is slower than the high-level, with fewer trajectories reaching as far east as South America. Most trajectories in each altitude range do not exhibit major vertical displacement during their 10 day journeys. Both the mid and high levels show that some parcels initialized near the equator re-circulate over Africa at the beginning of the period, consistent with *Garstang et al.* [1996]. Also, some parcels begin to circulate anticyclonically downstream near the end of the trajectory where the trajectory may be counted in a subsequent category. It is clear from these figures that the transport of pollutants from Africa can be rapid and over long distances.

Although the Australian (Figures 3b and 4b) and western Pacific (Figures 3c and 4c) transport categories each account for about 12% of the long-range trajectories, they exhibit different characteristics. The Australian category is due to circulation and subsidence around the quasi-stationary anticyclone west of Australia (Figure 1). Many trajectories at both high and mid levels subside to near the surface where wind speeds are light, with only a few eventually re-emerging from the anticyclone and continuing downstream during the 10 day period. As with the jet category, some trajectories initially move westward in an anticyclone over Africa before moving over the Indian Ocean.

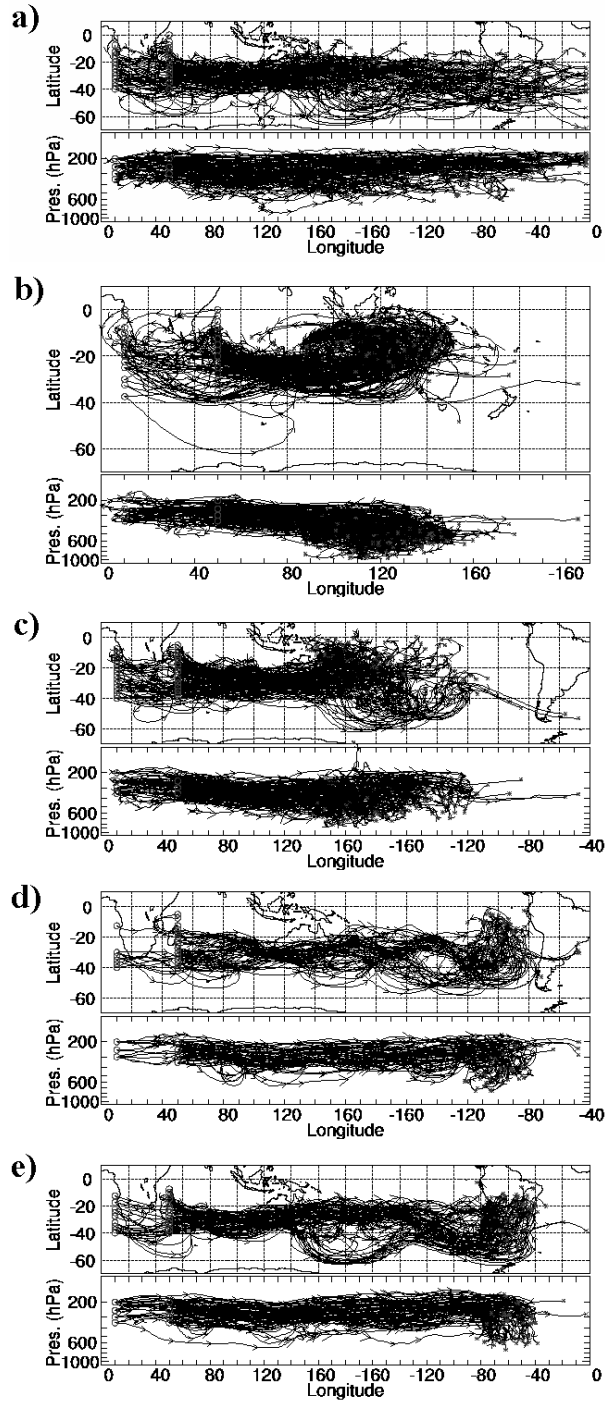


Figure 3. Ten-day forward trajectories initialized at 10°E and 50°E between 350 hPa and 200 hPa throughout the month of September 1996. The trajectories are separated into 5 transport categories: a) zonal, b) Australian anticyclonic, c) western Pacific anticyclonic, d) Easter Island anticyclonic, and e) South American anticyclonic. Between 100 and 200 representative trajectories are shown from each category. Circles indicate starting points; x's indicate ending points. The upper panel is a plan view; the lower is longitude vs. altitude (hPa).

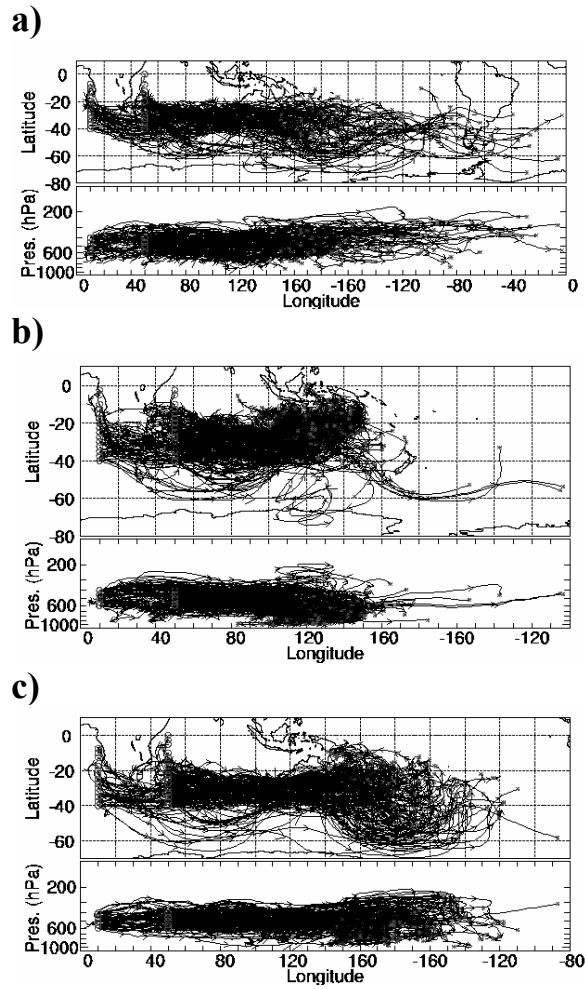


Figure 4. Ten-day forward trajectories as in Figure 3, but with starting altitudes between 600 hPa and 300 hPa. The three transport categories shown are: a) zonal, b) Australian anticyclonic, and c) western Pacific anticyclonic.

Conversely, the western Pacific transport category has a less distinct pathway, with transient anticyclones influencing trajectories over a wider latitude band from the equator as far south as 60°S. Few trajectories that begin at high levels descend to near the surface within 10 days, although some that are initialized at mid levels do extend to near the surface. As with the Australian category, some trajectories reach the tropics after 10 days or can re-emerge from a transient anticyclone and continue downstream. To summarize, burning byproducts that are involved in the Australian transport category would only reach the Pacific Basin after many additional days, if ever. The parcels then would be at lower altitudes where chemical depletion is relatively fast [Mauzerall *et al.*, 1998]. Plumes from Africa that reach the western Pacific transport category would be spread over a wide area consistent with the model simulation in Chatfield *et al.* [1998].

The remaining two anticyclonic transport categories from Africa are rarer, but more interesting in terms of anthropogenic pollution transport. The Easter Island category (Figure 3d) the South American category (Figure 3e) each account for only 2% of the 10-day long-range African trajectories. Only trajectories from the upper troposphere are shown for both cases, since less than 20 of the mid-level trajectories match either category. Both categories exhibit high altitude zonal transport during most of the 10 days, with subsidence and anticyclonic curvature at the end of the period.

The Easter Island and South American categories are examined more closely using quasi-Lagrangian trajectories starting at 180° (approximately 5 days transport from Africa) within the latitude and altitude bands at that longitude shown in Figures 3d and 3e, i.e., 15°S to 40°S and 500 hPa to 200 hPa. This approach (Figure 5) is preferable for illustrating the longer-term transport than are 15 day trajectories from Africa which would be more uncertain due to the longer time interval.

The quasi-permanent Easter Island anticyclone (Figure 1) is thought to be a major sink for pollution in the Pacific Basin [Hoell *et al.*, 1999]. And, the sample trajectories in Figure 5a indeed show that air at many altitudes and latitudes is affected by the anticyclone. Although a few trajectories re-emerge from the anticyclone and are transported over South America, most circulate in the anticyclone or move in the tropics for much of the 10 days depicted, which increases chemical depletion. The Easter Island

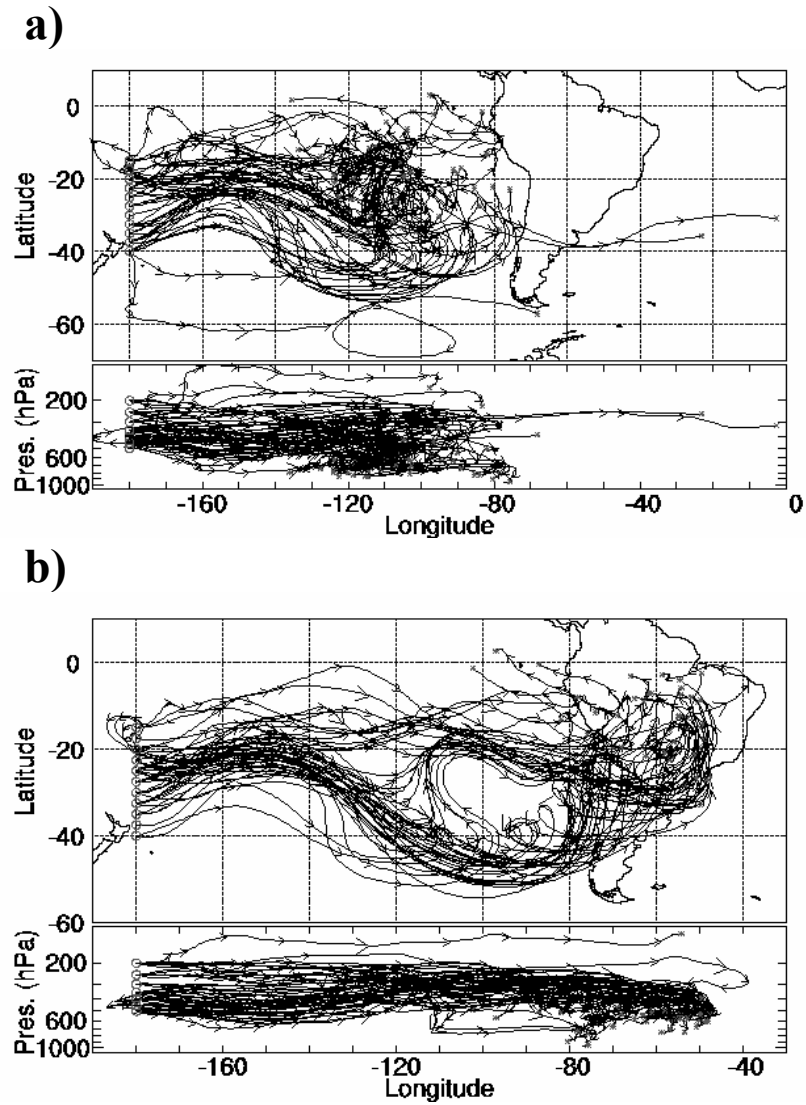


Figure 5. Ten-day forward trajectories initialized at 180° between 15°S and 40°S and 500 hPa and 200 hPa. Fifty sample trajectories from the two categories are shown: a) Easter Island anticyclonic and b) South American anticyclonic.

anticyclonic transport is analogous to the Northern Hemisphere “river of pollution” described by *Martin et al.* [2002]. The South American anticyclonic transport (Figure 5b) shows less subsidence during the 10 day period, with most descent occurring over the continent and not the eastern Pacific Ocean. Some trajectories eventually are transported back over the Pacific Ocean at lower altitudes. These trajectories show that air from Africa can be transported around the world to South America in 15 days, where biomass burning byproducts can affect the air quality over South America. In addition, the air can acquire additional byproducts from burning over South America itself [*Kirchhoff and Alvala*, 1996].

The five overlapping long-range transport categories described above account for 43% of the total 9180 trajectories in the data set. The remaining 57% of trajectories (not shown) do not experience long-range transport (reaching at least 110°E during the 10 days) for several reasons. Slow transport toward the Indian Ocean, especially close to the equator, is the main reason. However, many trajectories also recirculate in an anticyclone over Africa for some time, delaying their transport off the continent. Trajectories that intersect the prime meridian are terminated before they have a chance to recirculate eastward; however, *Garstang et al.* [1996] showed that very few of these trajectories do recirculate eastward within 10 days, and many move westward into the South Atlantic Basin. The number of current trajectories that end farther west than their starting point is 2183 out of 9180 or about 24% of the total.

In summary, trajectories during the PEM-Tropics A period confirm that long-range transport of air parcels from near Africa around the world is possible within 10 days. Since these trajectories were initialized between 600 hPa to the top of the troposphere, biomass burning byproducts must be lofted from surface fires by moist deep convection or other means. The terrain in southern Africa is relatively high, about 1.5 km above sea level, and on a hot day the mixing layer can reach well into the lower troposphere (3-4 km above sea level). However, once the air is lofted, the pollution not only can be transported long distances within 15 days, but also can subside back to the surface over Australia, the South Pacific Basin and South America.

3.2 Chemical Evolution during Transport

The chemical data collected during the two NASA campaigns describes an important aspect of transport from Africa to the Pacific Basin. The TRACE-A campaign was conducted near biomass burning sources in southern Africa and South America, while the PEM-Tropics A mission over the Pacific Ocean sampled the long-range downstream transport of these byproducts. The photochemical and physical dilution processes occurring during plume transport can be explored using mixing ratios of several NMHC's and CO which are emitted by the fires. Combining the chemical data with backward trajectories further elucidates the history of the pollution detected over the Pacific Ocean Basin.

To isolate the chemical samples having an African source from the complete PEM-Tropics A data set, clusters of 15 back trajectories were started every 5 min along the DC-8 and P-3B flight paths of each Southern Hemisphere flight during the campaign. If more than 8 points within a cluster passed within a box bounded by the equator and 40°S and the prime meridian and 40°E within 10 days of trajectory initiation, that 5 min period was considered to have an African origin. All samples collected during those 5 mins were included in the African data set. The age of the trajectory cluster is the mean time required to cross 40°E longitude (of those trajectories that did cross that longitude). An age of four days means that the average time is between 84 and 108 hours, 5 days is 108 to 132 hours, etc.

Out of the almost 30,000 total trajectories comprising the Southern Hemisphere flights, 1798 trajectories from 164 individual flight points were found to extend back to Africa, with ages between 4 and 8 days in the upper troposphere (arriving at the aircraft above 350 hPa), and 5 to 9 days in the mid-troposphere (arrivals between 600 and 350 hPa). These trajectories, sorted by days, are shown in Figures 6 (high) and 7 (mid). The high altitude arrivals in Figure 6 primarily depict zonal flow with little altitude change during transport, although the 6 day transport group (Figure 6c) is an exception, with many low level trajectories over Africa later lofting to high altitudes over the Pacific Ocean. The mid altitude arrivals show more variability in latitude along their trajectories, particularly in the 7, 8 and 9 day groups (Figures 7c, d and e). Many of the trajectories curve anticyclonically just before they are sampled along the flight path. There also is a

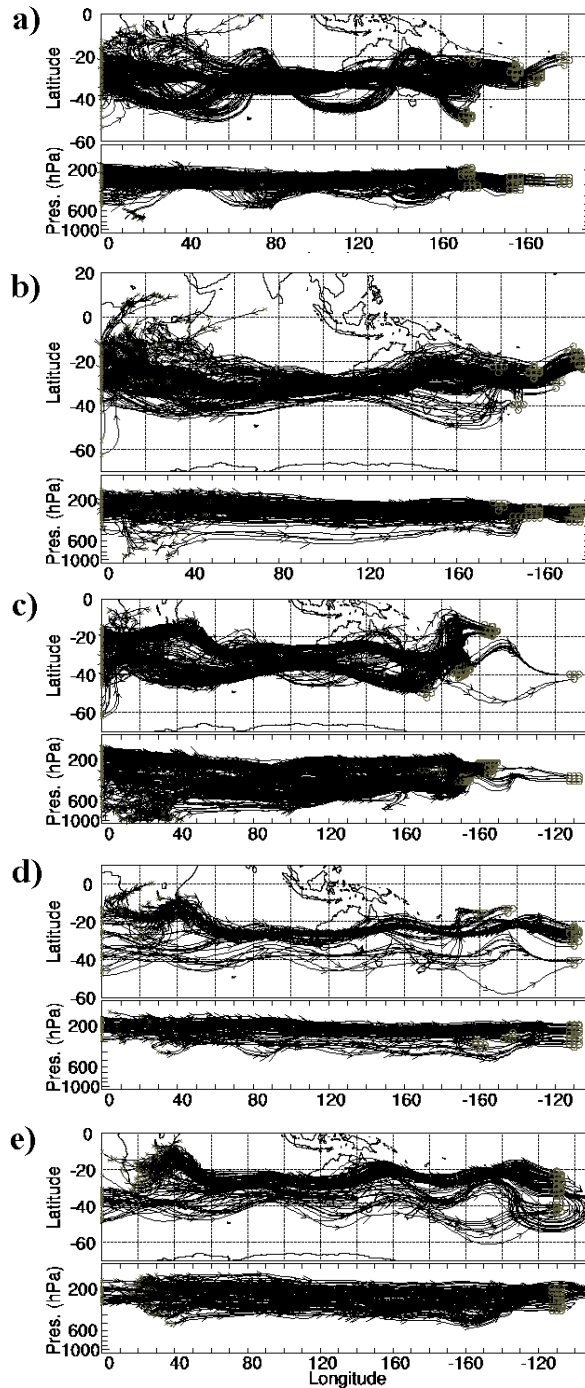


Figure 6. Ten day backward trajectories from PEM-Tropics A upper tropospheric flight paths (above 350 hPa) that extend back to Africa. Trajectories are grouped by the time required to reach Africa: a) 4 days, b) 5 days, c) 6 days, d) 7 days and e) 8 days.

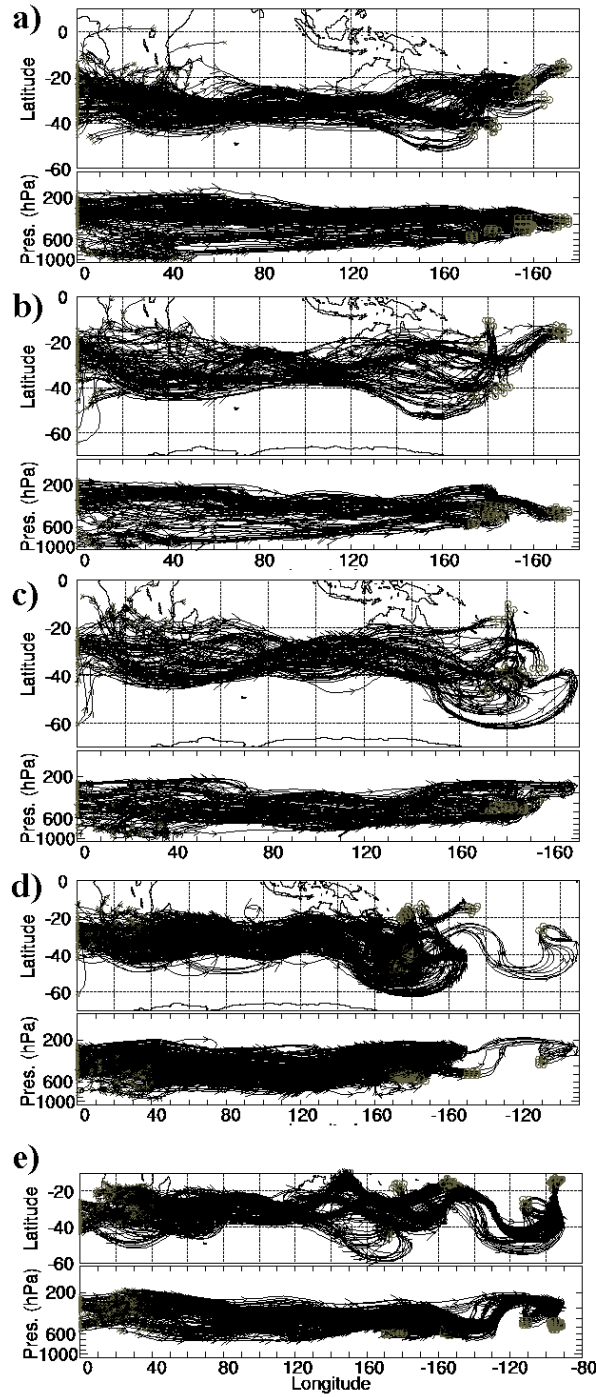


Figure 7. Ten day backward trajectories from PEM-Tropics A mid tropospheric flight paths (600 hPa to 350 hPa) that extend back to Africa. Trajectories are grouped by time required to reach Africa: a) 5 days, b) 6 days, c) 7 days, d) 8 days and e) 9 days.

wider altitude range within these trajectory groups, with trajectories passing over Africa from the ground level up to 200 hPa in the 5 and 6 day categories (Figures 7a, b).

The chemical composition of a plume depends on several factors, including the material being burned, the altitude of plume transport, and the length of time the plume is removed from its source. The timing based on the trajectories is more important for determining chemical characteristics than is distance from the source, because trajectories starting from similar longitudes can take different routes and/or experience different rates of transport. The number of days required to reach Africa for points along the flight paths is shown in Figure 8. While the time to reach locations near Easter Island (approximately 110°W) generally is longer than the time to reach points near New Zealand (approximately 175°E), the wide spatial distribution and overlapping of categories indicates that it would be erroneous to simply assume that the distance from a source is proportional to the time required to reach that source.

In addition to trajectories, certain hydrocarbons can be used to examine the samples' chemical age. Various hydrocarbons are photochemically decayed over different lifetimes, and they also are physically diluted through turbulent mixing in the atmosphere. *McKeen et al.* [1996] used simplified parameterizations of these processes to obtain a measure of their respective roles in diluting the species. The approach is to model the change in mixing ratio, X , with respect to time as:

$$\frac{dX}{dt} = -L_X X - K(X - X^B), \quad (1)$$

where t is time, L_X is the loss frequency of species X due to OH, X^B is the mixing ratio of X in the background air, and K is a coefficient that parameterizes all the physical processes that mix species X with the background. *McKeen et al.* mention several major simplifications used in this equation, including a strong dependence on the assumed background mixing ratio and assuming that mixing occurs only with air masses having the background mixing ratio. The background ratios used in the current study are shown in Table 2. The procedure used to obtain the background values are described later. Using the ratio of two different species, equation (1) can be solved for the limiting cases of pure mixing or pure photochemical depletion by eliminating time and/or the parameter K . The observed chemical data should fall between these limiting cases.

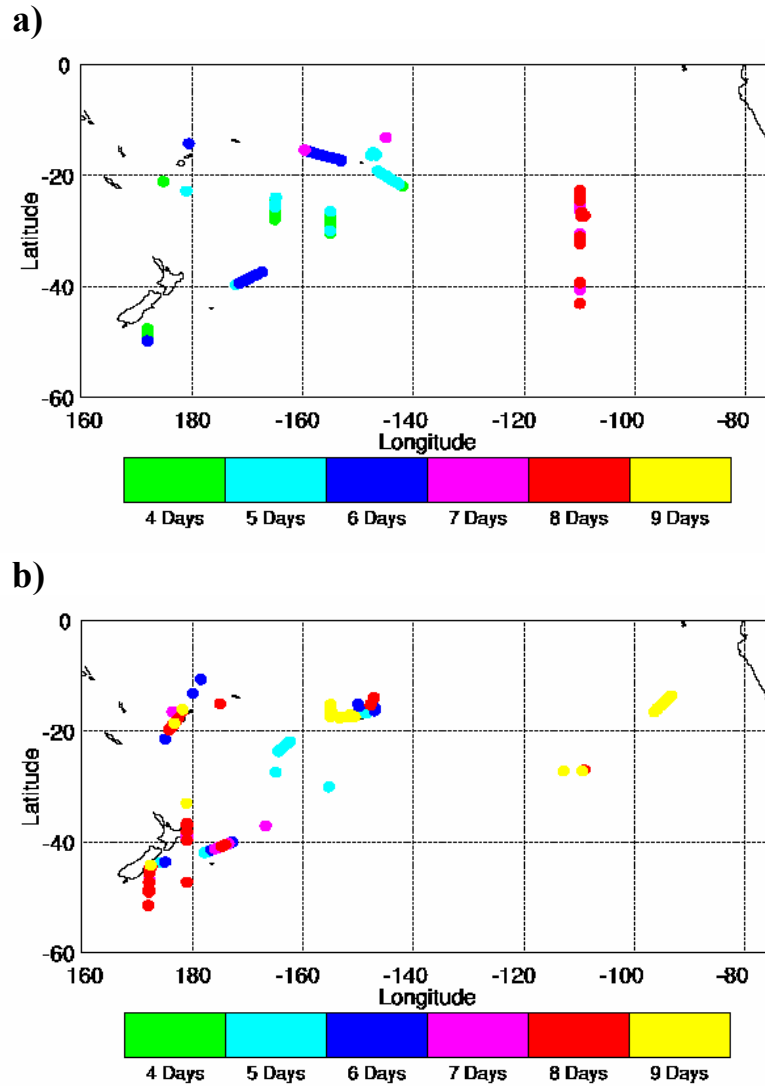


Figure 8. Locations of points along flight tracks during PEM-Tropics A from which backward trajectories reach Africa during various time intervals (color bar) for a) upper tropospheric and b) mid tropospheric flight segments.

Table 2. Mean values for species from groupings discussed in Figures 9 through 14.

	<i>Propane</i> (pptv)	<i>Ethane</i> (pptv)	<i>CO</i> (ppbv)	<i>Ethyne</i> (pptv)
High Trop				
TRACE-A	87	727	103	133
4-5 days	35	494	72	82
6-7 days	31	407	65	75
8 days	24	404	57	50
Background	10	213	42	21
Mid Trop				
TRACE-A	56	660	107	149
5-6 days	46	638	93	139
7-8 days	35	533	94	122
9 days	28	486	76	85
Background	13	263	52	22

Figures 9 and 10 show log-log correlation plots for ethane and propane for high tropospheric arrival altitudes and mid-tropospheric arrival altitudes, respectively. The top panels show all of the African data sorted by transport time as well as the TRACE-A data. The TRACE-A data are included since they are expected to have a much shorter age than those from PEM-Tropics A. The TRACE-A data consist of all values detected above 350 hPa, regardless of whether they were sampled over southern Africa, South America or the South Atlantic Ocean. Also plotted as an asterisk, for comparison, are the values of propane and ethane detected while at low levels close to a burning source [Mauzerall *et al.*, 1998]. The limiting cases described above are plotted with the dashed dotted line representing pure photochemical decay and the solid line pure physical dilution. A least squares best fit regression line based on the combination of all the PEM-Tropics A and TRACE-A data is plotted as well (dashed). The intersection of the three lines is on the best fit regression line at the greatest observed value of propane. The lower panels show the same three lines for reference, as well as mean values for the TRACE-A data and the 2 day groupings of the PEM-Tropics data. Numerical values of these means are given in Table 2.

The strong relationship between ethane and propane can be seen in Figures 9 and 10. These NMHC's, as well as ethyne, have longer photochemical lifetimes than most species used in previous studies [e.g., Mauzerall *et al.*, 1998; McKeen *et al.* 1996], and are best suited for examining long-range transport. Almost all the observed data are within the limiting cases. The wide range of propane in the TRACE-A data at high altitudes, between approximately 10 pptv to 1041 pptv, shows a much fresher influence than the PEM-Tropics A data, which ranges from approximately 10 pptv to 63 pptv. The TRACE-A mid altitude layer does not exhibit as wide a range for propane, with 323 pptv being the largest value. However, propane does display more range in the PEM-Tropics A data set, 11 pptv to 113 pptv. The sample taken near a burning source (the asterisk, [Mauzerall *et al.*, 1998]) is close to the greatest value of ethane measured at both altitudes, but much weaker than the propane values sampled at high altitudes during TRACE-A. The orientation of the best fit line shows that both physical mixing and photochemical dilution are important in the overall dilution of these two species in both altitude layers. The means (lower panels) show the expected logarithmic decay in the

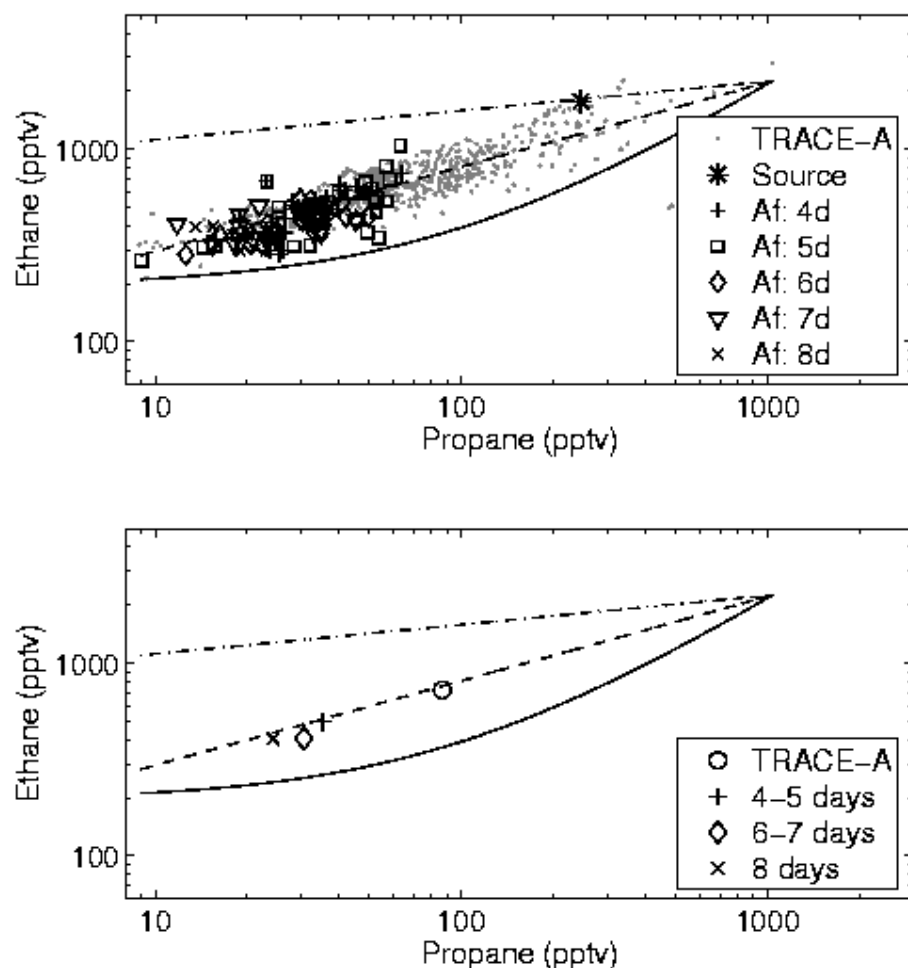


Figure 9. Correlation plot of ethane versus propane for high altitudes (above 350 hPa) for all TRACE-A data and PEM-Tropics A data corresponding to trajectories in Figure 6. The upper panel shows all values; the small gray dots are TRACE-A data; the asterisk is values collected during TRACE-A at low altitudes near a biomass burning source [from *Mauzerall et al., 1998*]. The solid line is the expected relationship based only physical mixing of inert species; the dashed-dotted line is the relationship based only on OH scavenging. The dashed line is the regression fit through all data points. The intersection of the lines is along the regression line at the greatest observed value of propane. The lower panel shows mean values for PEM-Tropics A 2 day groupings and the TRACE-A data set as well as the lines from the upper panel.

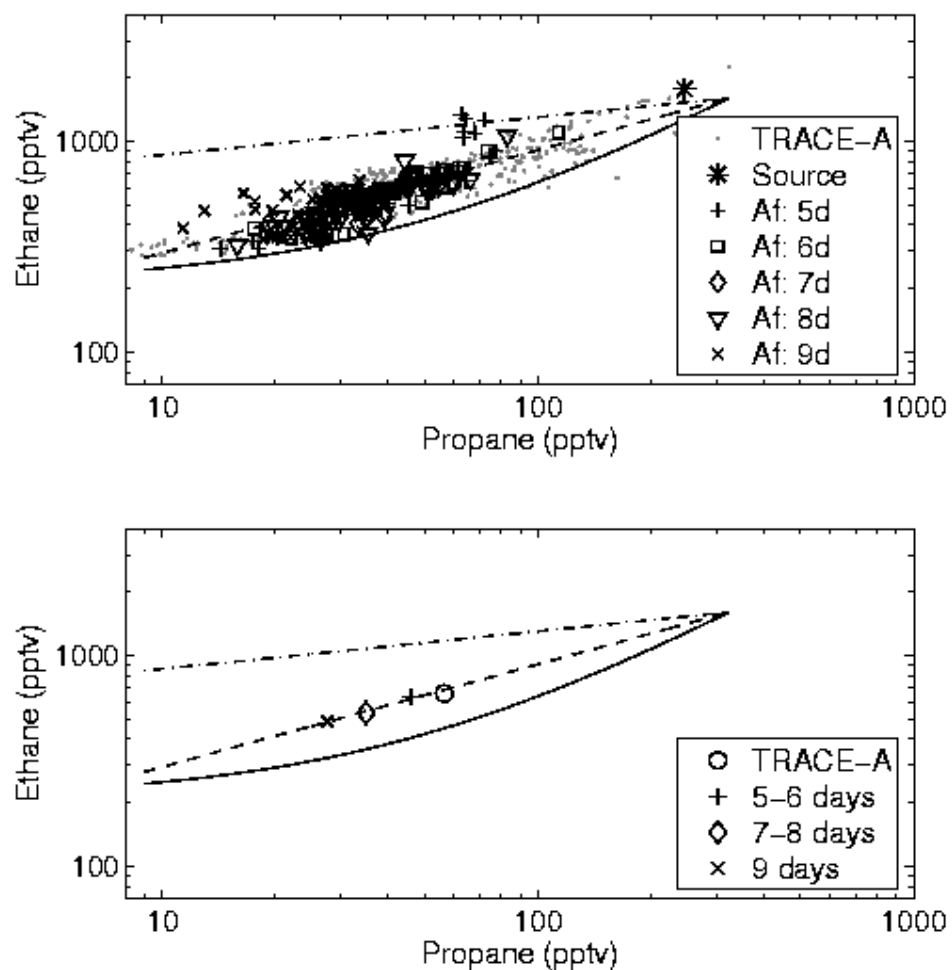


Figure 10. As in Figure 9, but a correlation plot of ethane versus propane for mid tropospheric collection levels, 600 hPa to 350 hPa. The lines and points have the same meaning as in Figure 9.

two species. The individual days show variability in the samples, with values near background levels in some cases. This is partially due to the intermittent nature of the initial vertical transport from the surface fires to the higher altitudes where the main horizontal transport off the African continent occurs, meaning that some trajectories that passed over Africa did not incorporate pollutants, probably due to insufficient burning and/or vertical transport near the burning sources.

To further investigate the roles of mixing and photochemical decay, the species ethyne and CO are plotted at high and mid levels (Figures 11 and 12, respectively). Individual values generally are very close to the best fit regression line, although at high altitudes the PEM-Tropics A CO data are slightly less than the corresponding TRACE-A CO values. This probably is due to the background mixing ratios for CO being greater over the South Atlantic during the TRACE-A mission due to the recirculation around the South Atlantic anticyclone [Blake *et al.*, 1996]. Thus, CO, which is both a primary product from fires and a secondary product from atmospheric oxidation, had time to build up during the burning season and shifted the background values. This shift causes the mean trajectory-derived transport time for PEM-Tropics A to be below the best fit line in the lower panel of Figure 11. The sample collected near the biomass burning source in TRACE-A exhibits greater values of CO and ethyne than the upper-level TRACE-A samples. Also, unlike the propane to ethane ratio means in Figures 9 and 10, the ethyne to CO ratio means (lower panels) are not as evenly spaced on the log-log plot. In fact, Table 2 shows the mid-level 7-8 day category mean CO value is greater by 1 ppbv than the 5-6 day category mean. This is caused by a few major outliers in the 8 day group that exhibit large values of CO and ethyne. These large values may be due to a fresher influence from Australia, which has few fires (Figure 2) but is along the trajectory pathway, or by uncertainties in the trajectories themselves.

Ethyne and ethane is the last pair of species to be investigated [Figures 13 (high levels) and 14 (mid levels)]. These species display greater scatter than the previous pairs of species, most likely because they can have different sources, whereas the CO and ethyne pair and the propane and ethane pair have similar biomass burning sources [Talbot *et al.*, 1996]. The cluster of large ethane values near 100 pptv of ethyne in the TRACE-A data at high levels (Figure 13, top panel) immediately suggests a different source. The

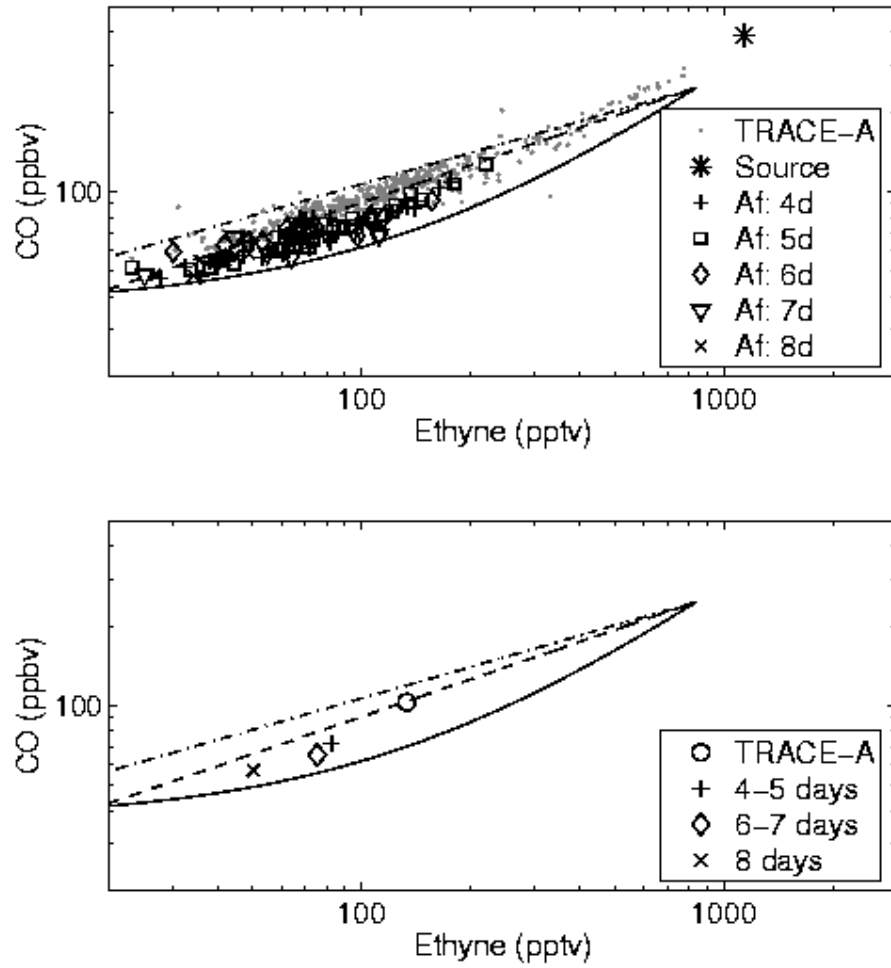


Figure 11. As in Figure 9, but a correlation plot of CO versus ethyne for upper tropospheric levels. The lines and points have the same meaning as in Figure 9.

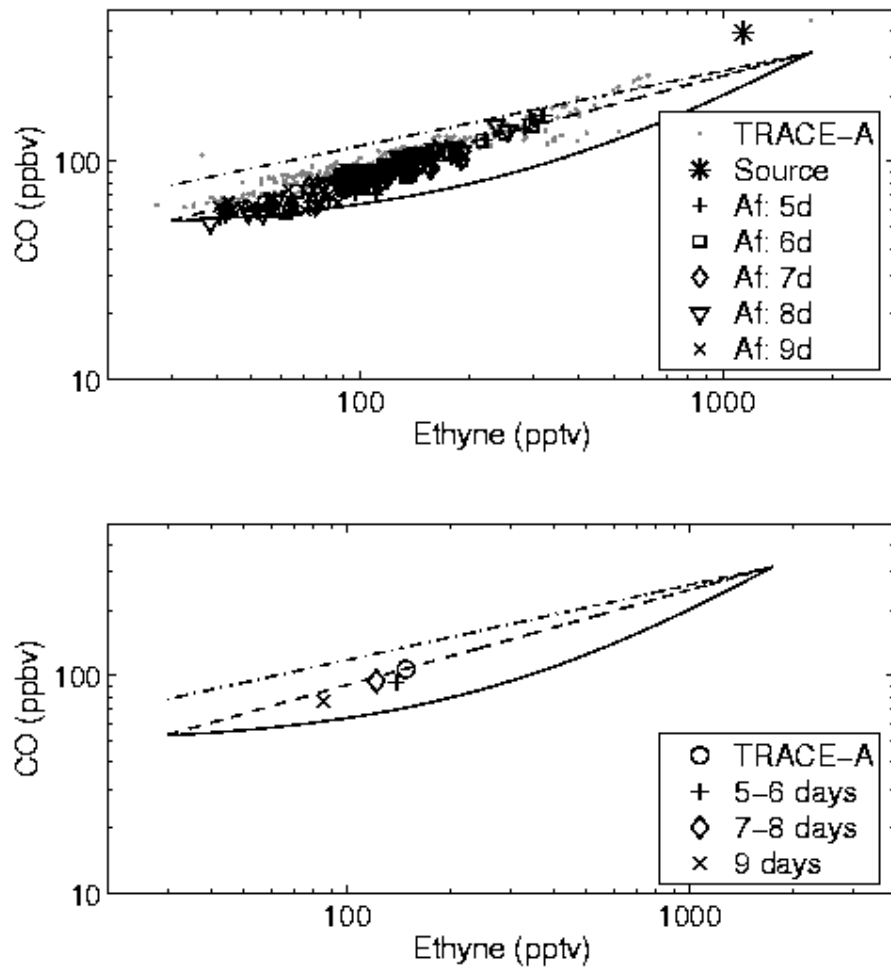


Figure 12. As in Figure 9, but a correlation plot of CO versus ethyne for mid tropospheric levels. The lines and points have the same meaning as in Figure 9.

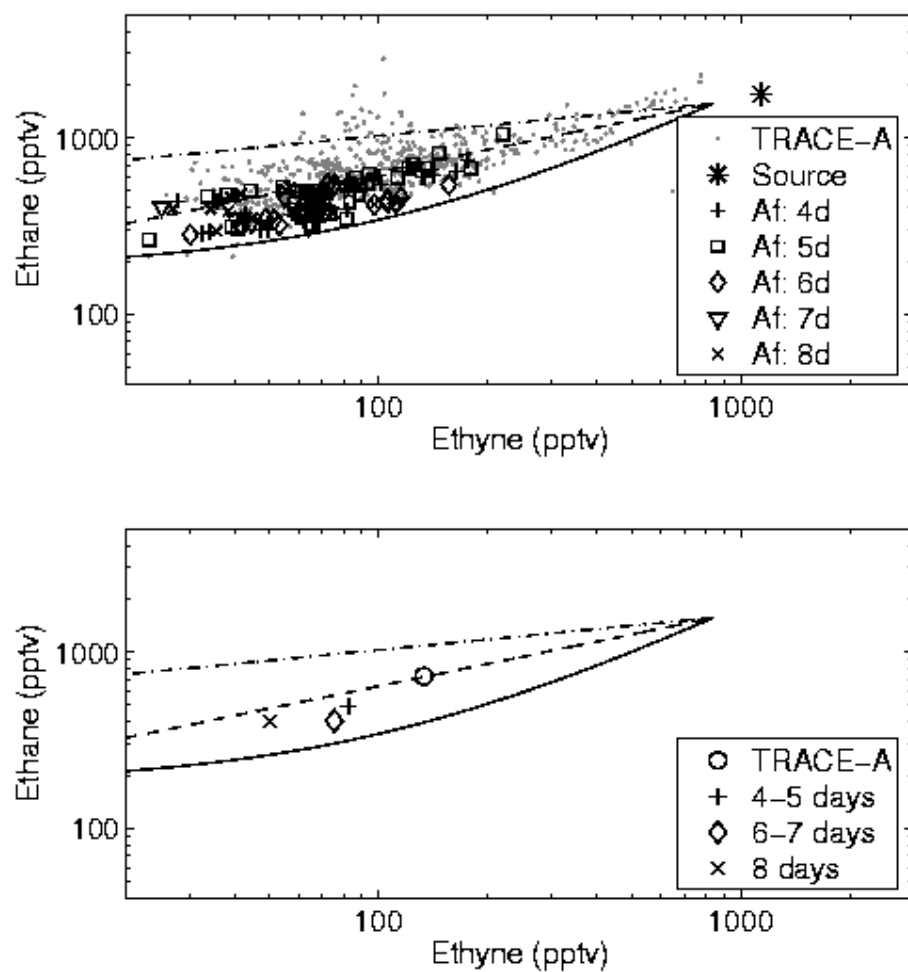


Figure 13. As in Figure 9, but a correlation plot of ethane versus ethyne for upper tropospheric levels. The lines and points have the same meaning as in Figure 9.

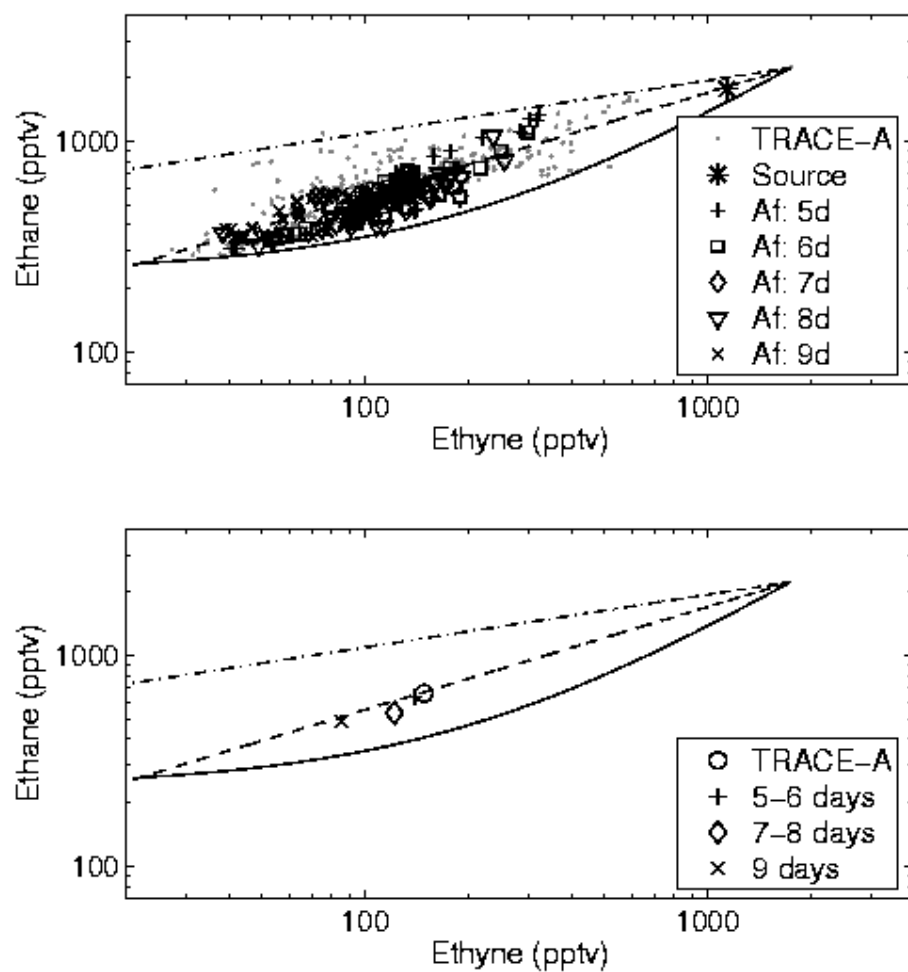


Figure 14. As in Figure 9, but a correlation plot of ethane versus ethyne for mid tropospheric levels. The lines and points have the same meaning as in Figure 9.

location of the samples as well as backward trajectories indicate that this air passed over South America, not Africa, and may represent industrial sources instead of biomass burning [Talbot *et al.*, 1996]. These large values bias the slope of the regression line above the mean values for the PEM-Tropics A data. This scatter is not evident on the mid-level plot, which is better correlated. As noted with CO and ethyne (Figures 11 and 12), the mean daily values are not evenly spaced on the log-log plots, although they do diminish with time.

In comparing the plots of high altitude versus middle altitude values for the three pairs of species (Figures 9 to 14), the relative location of the TRACE-A means to the three PEM-Tropics A mean values is noteworthy. Specifically, the TRACE-A mean on the high altitude plots is much greater than the three PEM-Tropics A means, but the TRACE-A mean is more similar to the other three in the mid altitude plots. In addition, comparisons within the campaign data sets show that mid altitude mean values of mixing ratios for PEM-Tropics A are greater than high altitude means (Table 2). The TRACE-A mid altitude mean values are smaller than or equivalent to high altitude values. These relations suggest that deep vertical transport near the source area, such as by moist convection, rapidly lofts pollution to the high troposphere through outflow near the cloud tops [e.g., Pickering *et al.*, 1996], but that “exhaust” to mid altitude levels is not as strong. However, at long ranges more pollution is transported in the mid troposphere, since air can both sink from higher altitudes or be lofted slowly from low altitudes during transport.

It is informative to examine the value of the physical mixing lifetime, K from equation (1). This is a measure of the exponential decay towards a background value due to mixing with the background air. This parameter can be approximated by integrating equation (1) and using mean values for the 2 day groups as a measure of the temporal change in the mixing ratio. The equation:

$$X_2 = \frac{KX^B}{K + L_X} + \left(X_1 - \frac{KX^B}{K + L_X} \right) e^{-(K+L_X)t}, \quad (2)$$

must be solved iteratively for K . We used mean values for the 4/5 day and 8 day groups for X_1 and X_2 , respectively, to estimate the high tropospheric mixing lifetime, and the 5/6 day and 9 day groups to estimate the mid troposphere mixing lifetime. Results for each

of the four species examined are shown in Table 3. These results are only estimates since there are many uncertainties in this approach beyond the simplifications to K mentioned earlier. Specifically, this equation is very sensitive to uncertainties in the assumed photochemical lifetimes and in the background mixing ratios (Table 2), both of which were estimated based on the entire PEM-Tropics A data. The background mixing ratios for the mid troposphere were defined as the 10th percentile of a cumulative distribution function (CDF) for the mid levels. The upper tropospheric background mixing ratios assume some mixing from stratospheric air, so the mixing ratio is defined as the 10th percentile from a CDF of the upper tropospheric points averaged with a mean of the stratospheric points. The varied results for the upper troposphere, approximately 4.5 days difference between the estimated mixing lifetimes for ethane (10.5 days) and propane (11.3 days) as opposed to CO (6.6 days) and ethyne (6.5 days), suggest that uncertainties lead to larger errors at high levels than at mid levels. The mid-level mixing lifetimes are more similar, approximately 8.5 days. Both the mid-level and upper-level mixing lifetimes are shorter than the shortest photochemical lifetime of the species being examined: propane, approximately 15 days. This relatively shorter lifetime suggests that physical mixing at long ranges is more important to dilution of long-lived species than is photochemical dilution.

Table 3. Physical mixing lifetime calculated from equation (2) for the four species used in this study.

	<i>Propane</i>	<i>Ethane</i>	<i>CO</i>	<i>Ethyne</i>
Upper Trop	11.3 days	10.5 days	6.6 days	6.5 days
Mid Trop	8.4 days	8 days	9.2 days	8.6 days

CHAPTER 4

SUMMARY AND CONCLUSIONS

This study has examined the pathways and chemical evolution that occur during atmospheric transport from Africa into the Pacific Basin. Data from two NASA campaigns, TRACE-A and PEM-Tropics A, were used during the austral spring months when biomass burning is widespread in the Southern Hemisphere. Specifically, long-range transport during September 1996 was examined using forward trajectories bracketing Africa, as well as backward trajectories that reached Africa from locations along the DC-8 and P-3B flight paths during PEM-Tropics A. Long-range transport was defined as forward trajectories reaching at least 110°E within 10 days.

Results showed that long-range transport from Africa could be grouped into five major (overlapping) categories that contain 43% of the total 10 day forward trajectories: zonal flow and anticyclonic transport over Australia, the western Pacific, Easter Island and South America. The remaining 57% of trajectories were not considered long-range as they did not reach 110°E. The majority of the long-range transport occurred in zonal flow, with transport around the Australian anticyclone and the western Pacific transient anticyclones being next most prevalent. Less than 2% of trajectories experienced anticyclonic flow over Easter Island and South America within 10 days of leaving Africa. However, within 15 days of passing over Africa, transport around the Easter Island anticyclone and the South American anticyclone could result in pollutants incorporated over Africa subsiding to near the surface. Air passing over South America could pick up additional pollution due to biomass burning over that continent.

The chemical evolution occurring during long-range transport from Africa was examined using chemical data collected during the two field campaigns. Determining the relative roles of photochemical decay and physical mixing was emphasized. Trajectory cluster analysis extracted 164 five min flight segments whose backward trajectories

passed over Africa within 10 days prior to being sampled during the PEM-Tropics A mission. The length of time between passing over Africa and in situ sampling in the upper troposphere over the Pacific was found to range from 4 to 8 days. In the mid troposphere these transport times ranged from 5 to 9 days. These parcels originating over Africa were compared to TRACE-A samples collected near the source areas using procedures similar to those of *McKeen et al.* [1996]. This technique also reveals the limiting cases for photochemical decay and simplified physical mixing.

Correlation plots of ethane vs. propane, CO vs. ethyne and ethane vs. ethyne showed that the samples mostly fell between the limiting cases. An exception was in the ethane vs. ethyne plot for TRACE-A data that probably was due to air having a non-African source. In general, 2 day means for the PEM-Tropics A samples exhibited the expected exponential decay, although not always uniformly. Best fit regression lines to the data indicated that both photochemical decay and physical mixing are important in the dilution of pollution from Africa. To our knowledge, this is the first combination of these approaches since *McKeen et al.* [1996], particularly for upper tropospheric data.

Comparisons between the high altitude and mid altitude mean mixing ratios suggested that vertical transport near the source lofts more biomass burning byproducts to high altitudes. However, at long ranges and times more pollutants are transported to mid altitude levels. Typical mixing lifetimes were found to be shorter than photochemical lifetimes for the species. The maximum estimated mixing lifetime was 11.5 days and the shortest was 6.5 days. Upper-level mixing lifetimes had more variability than mid-level mixing lifetimes, which were approximately 8.5 days for all species. The physical mixing lifetime for all species was shorter than the photochemical decay lifetime, suggesting that physical mixing is more important to dilution than photochemical decay.

Our combination of trajectories and chemical data clarifies the overall African transport scenario. These results are consistent with those from earlier studies [e.g., *Staudt et al.*, 2002; *Singh et al.*, 2000; *Chatfield et al.*, 2002]. Air parcels from different altitudes over Africa are transported over the Pacific Basin at various speeds. During this transport the various species are diluted both by photochemical decay and also by physical mixing with background air.

No chemical data are available at locations further downstream of the current sampling sites. However, forward trajectories from the sampling locations in Figures 6 and 7 (Figure 15) suggest where the air parcels would be within 10 days after being sampled during the PEM-Tropics A campaign. The upper tropospheric arrivals (Figure 15a) mostly remain in the upper levels, although a few trajectories descend anticyclonically over Easter Island and South America. However, the mid tropospheric arrivals (Figure 15b) demonstrate all five transport categories described above, i.e., zonal transport to the prime meridian, anticyclonic descent over the western and eastern Pacific and South America. A few trajectories move at low altitudes over Australia.

The current results show that pollution produced through biomass burning over the African continent is not confined to the Atlantic and Indian Oceans, but can travel around the world within 10 days. Within 15 to 20 days, shorter than most of the photochemical lifetimes of species used in this study, pollution can descend to near the surface of South America and the remote tropical Pacific where photochemical depletion is faster. Although biomass burning byproducts can affect air quality far downstream from burning sources, the tropical Pacific Ocean also is an effective sink of pollution as photochemical depletion is greater in the tropics than the mid-latitudes due to greater sunlight and water vapor.

It would be ideal if future studies of pollution from Africa would collect in situ data over even longer ranges that span the entire globe. Although this is not practical during aircraft campaigns, satellite-derived chemical estimates and geochemical models are well suited for remote sensing or simulating global scale transport processes.

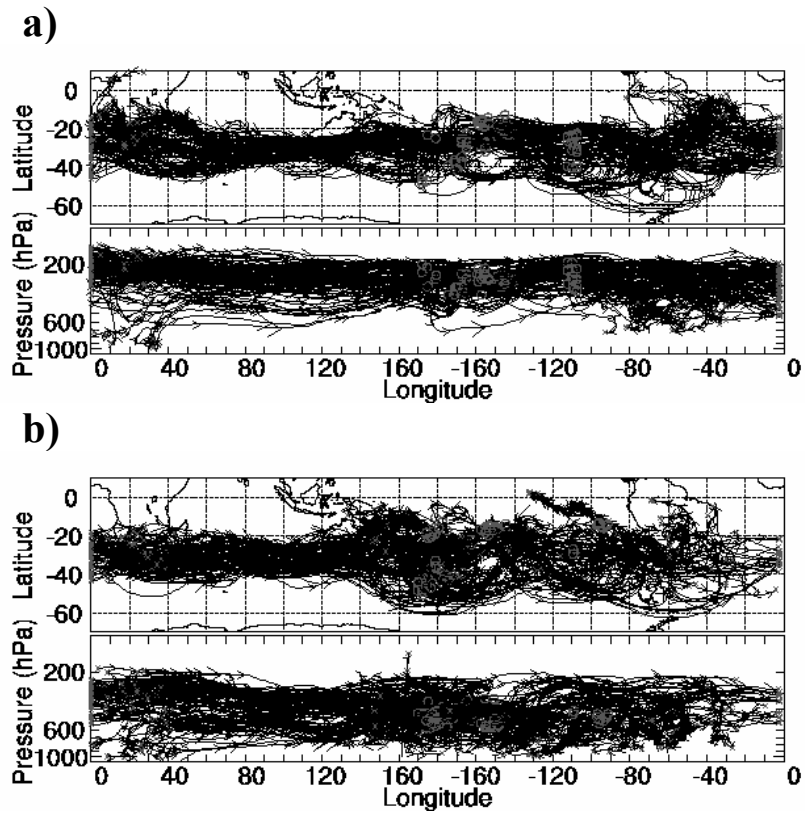


Figure 15. Ten-day backward and ten-day forward trajectories from the sampling locations in Figure 6, upper troposphere (a) and Figure 7, mid troposphere (b). Only approximately 100 representative trajectories are shown.

REFERENCES

- Bethan, S., G. Vaughan, C. Gerbig, A. Volz-Thomas, H. Richer, D.A. Tiddeman, Chemical air mass differences near fronts, *J. Geophys. Res.*, *103*, 13413-13434, 1998.
- Blake, N. J., D. R. Blake, B. C. Sive, T.-Y. Chen, F. S. Rowland, J. E. Collins, Jr., G. W. Sachse, and B. E. Anderson, Biomass burning emissions and vertical distribution of atmospheric methyl halides and other reduced carbon gases in the South Atlantic region, *J. Geophys. Res.*, *101*, 24151-24164, 1996.
- Blake, N. J., D. R. Blake, O. W. Wingenter, B. C. Sive, L. M. McKenzie, J. P. Lopez, I. J. Simpson, H. E. Fuelberg, G. W. Sachse, B. E. Anderson, G. L. Gregory, M. A. Carroll, G. M. Albercook, and F. S. Rowland, Influence of southern hemispheric biomass burning on midtropospheric distributions of nonmethane hydrocarbons over the remote South Pacific, *J. Geophys. Res.*, *104*, 16213-16232, 1999.
- Board, A. S., H. E. Fuelberg, G. L. Gregory, B. G. Heikes, M. G. Schultz, D. R. Blake, J. E. Dibb, S. T. Sandholm, and R. W. Talbot, Chemical characteristics of air from differing source regions during the Pacific Exploratory Mission-Tropics A (PEM-Tropics A), *J. Geophys. Res.*, *104*, 16181-16196, 1999.
- Chatfield, R. B., J. A. Vastano, L. Li, G. W. Sachse, and V. S. Connors, The Great African Plume from biomass burning: Generalizations from a three-dimensional study of TRACE-A carbon monoxide, *J. Geophys. Res.*, *103*, 28059-28077, 1998.
- Chatfield, R.B., Z. Guo, G. W. Sachse, D. R. Blake, N. J. Blake, The subtropical global plume in the Pacific Exploratory Mission- Tropics A (PEM-Tropics A), PEM-Tropics B, and the Global Atmospheric Sampling Program (GASP): How tropical emissions affect the remote Pacific, *J. Geophys. Res.*, *107*, doi:10.1029/2001JD000497, 2002.
- Dibb, J. E., R. W. Talbot, L. D. Meeker, E. M. Scheuer, N. J. Blake, D. R. Blake, G. L. Gregory, and G. W. Sachse, Constraints on the age and dilution of Pacific Exploratory Mission-Tropics biomass burning plumes from the natural radionuclide tracer ^{210}Pb , *J. Geophys. Res.*, *104*, 16,233-16,241, 1999.
- Fenn, M. A., E. V. Browell, C. F. Butler, W. B. Grant, S. A. Kooi, M. B. Clayton, G. L. Gregory, R. E. Newell, Y. Zhu, J. E. Dibb, H. E. Fuelberg, B. E. Anderson, A. R. Bandy, D. R. Blake, J. D. Bradshaw, B. G. Heikes, G. W. Sachse, S. T.

- Sandholm, H. B. Singh, R. W. Talbot, and D. C. Thornton, Ozone and aerosol distributions and air mass characteristics over the South Pacific during the burning season, *J. Geophys. Res.*, *104*, 16197-16212, 1999.
- Fishman, J., J. M. Hoell, Jr., R. J. Bendura, R. J. McNeal, and V. W. J. H. Kirchhoff, NASA GTE TRACE-A experiment (September-October, 1992): Overview, *J. Geophys. Res.*, *101*, 23865-23880, 1996.
- Fuelberg, H. E., R. O. Loring, Jr., M. V. Watson, M. C. Sinha, K. E. Pickering, A. M. Thompson, G. W. Sachse, D. R. Blake, and M. R. Schoeberl, TRACE-A trajectory intercomparison: 2, Isentropic and kinematic methods, *J. Geophys. Res.*, *101*, 23927-23939, 1996.
- Fuelberg, H. E., R. E. Newell, S. P. Longmore, Y. Zhu, D. J. Westberg, E. V. Browell, D. R. Blake, G. L. Gregory, and G. W. Sachse, A meteorological overview of the Pacific Exploratory Mission (PEM) Tropics period, *J. Geophys. Res.*, *104*, 5585-5622, 1999.
- Fuelberg, H. E., J. R. Hannan, P. F. J. van Velthoven, E. V. Browell, G. Bieberbach, Jr., R. D. Knabb, G. L. Gregory, K. E. Pickering, and H. B. Selkirk, A meteorological overview of the SONEX period. *J. Geophys. Res.*, *105*, 3633-3651, 2000.
- Garstang, M., P. D. Tyson, R. Swap, M. Edwards, P. Kallberg, J. A. Lindesay, Horizontal and vertical transport of air over southern Africa, *J. Geophys. Res.*, *101*, 23721-23736, 1996.
- Gregory, G. L., H. E. Fuelberg, S. P. Longmore, B. E. Anderson, J. E. Collins, Jr., and D. R. Blake, Chemical characteristics of tropospheric air over the tropical South Atlantic Ocean: Relationship to trajectory history, *J. Geophys. Res.*, *101*, 23957-23972, 1996.
- Hannan, J. R., H. E. Fuelberg, A. M. Thompson, G. Bieberbach, Jr., R. D. Knabb, Y. Kondo, B. E. Anderson, E. V. Browell, G. L. Gregory, G. W. Sachse, and H. Singh, Atmospheric chemical transport based on high resolution model-derived winds: A case study, *J. Geophys. Res.*, *105*, 3807-3820, 2000.
- Hao, W. M., D. E. Ward, G. Olbu, S. P. Baker, Emissions of CO₂, CO, and hydrocarbons from fires in diverse African savanna ecosystems, *J. Geophys. Res.*, *101*, 23577-23584, 1996.
- Hurrell, J.W., H. van Loon, D.J. Shea, The mean state of the troposphere, in *Meteorology of the Southern Hemisphere*, edited by D.J. Karoly and D.G. Vincent, pp 1-46, American Meteorological Society, Boston, Mass., 1998.
- Hoell, J. M., D. D. Davis, D. J. Jacob, M. O. Rodgers, R. E. Newell, H. E. Fuelberg, R. J. McNeal, J. L. Raper, and R. J. Bendura, Pacific Exploratory Mission in the

- tropical Pacific: PEM-Tropics A, August-September 1996, *J. Geophys. Res.*, *104*, 5567-5583, 1999.
- Kirchhoff, V. W. J. H., and P. C. Alvala, Overview of an aircraft expedition into the Brazilian cerrado for the observation of atmospheric trace gases, *J. Geophys. Res.*, *101*, 23973-23982, 1996.
- Lusher, W.R., An examination of atmospheric transport during the Pacific Exploratory Mission – Tropics, Master's Thesis, Dept. of Meteorology, Florida State University, 1999.
- Martin, B.D., H. E. Fuelberg, N. J. Blake, J. H. Crawford, J. A. Logan, D. R. Blake, G. W. Sachse, Long-range transport of Asian outflow to the equatorial Pacific, *J. Geophys. Res.*, *107*, 8322, doi:10.1029/2001JD001418, 2002.
- Mauzerall, D. L., J. A. Logan, D. J. Jacob, B. E. Anderson, D. R. Blake, J. D. Bradshaw, B. G. Heikes, G. W. Sachse, H. B. Singh, and R. W. Talbot, Photochemistry in biomass burning plumes and implications for tropospheric ozone over the tropical South Atlantic, *J. Geophys. Res.*, *103*, 8401-8423, 1998.
- McKeen, S.A. and S.C. Liu, Hydrocarbon ratios and photochemical history of air masses, *Geophys. Res. Lett.*, *20*, 2362-2366, 1993.
- McKeen, S. A., S. C. Liu, E.-Y. Hsie, X. Lin, J. D. Bradshaw, S. Smyth, G. L. Gregory and D. R. Blake, Hydrocarbon ratios during PEM-West A: A model perspective, *J. Geophys. Res.*, *101*, 2087-2109, 1996.
- Newell, R. E., J.W. Kidson, D. G. Vincent, and G. J. Boer, *The General Circulation of the Tropical Atmosphere and Interactions with Extratropical Latitudes, Vol. 1*, Dept. of Meteorology, Massachusetts Institute of Technology, 258 pp., 1972.
- Olson, J. R., B. A. Baum, D. R. Cahoon, and J. H. Crawford, Frequency and distribution of forest, savanna, and crop fires over tropical regions during PEM-Tropics A, *J. Geophys. Res.*, *104*, 5865-5876, 1999.
- Pickering, K. E., A. M. Thompson, Y. Wang, W.-K. Tao, D. P. McNamara, V. W. J. H. Kirchhoff, B. G. Heikes, G. W. Sachse, J. D. Bradshaw, G. L. Gregory, and D. R. Blake, Convective transport of biomass burning emissions over Brazil during TRACE-A, *J. Geophys. Res.*, *101*, 23993-24012, 1996.
- Schultz, M. G., D. J. Jacob, Y. Wang, J. A. Logan, E. L. Atlas, D. R. Blake, N. J. Blake, J. D. Bradshaw, E. V. Browell, M. A. Fenn, F. Flocke, G. L. Gragory, B. G. Heikes, G. W. Sachse, S. T. Sandholm, R. E. Shetter, H. B. Singh, and R. W. Talbot, On the origin of tropospheric ozone and NO_x over the South Pacific, *J. Geophys. Res.*, *104*, 5829-5843, 1999.

- Singh, H. B., W. Viezee, Y. Chen, J. Bradshaw, S. Sandholm, D. Blake, N. Blake, B. Heikes, J. Snow, R. Talbot, E. Browell, G. Gregory, G. Sachse, S. Vay, Biomass burning influences on the composition of the remote South Pacific troposphere: analysis based on observations from PEM-Tropics A, *Atmos. Environ.* *34*, 645-644, 2000.
- Staudt, A. C., D. J. Jacob, J. A. Logan, D. Bachiochi, T. N. Krishnamurti, N. Poisson, Global chemical model analysis of biomass burning and lightning influences over the South Pacific in austral spring, *J. Geophys. Res.*, *107*, doi:10.1029/2000JD000296, 2002.
- Stohl, A., G. Wotawa, P. Seibert, H. Kromp-Kolb, Interpolation errors in wind fields as a function of spatial and temporal resolution and their impact on different types of kinematic trajectories, *J. Appl. Meteorol.*, *34*, 2149-2165, 1995.
- Stohl, A., and P. Seibert, Accuracy of trajectories as determined from conservation of meteorological tracers, *Q. J. R. Meteorol. Soc.*, *124*, 1465-1484, 1998.
- Stohl, A., and T. Trickl, A textbook example of long-range transport: Simultaneous observation of ozone maxima of stratospheric and North American origin in the free troposphere over Europe. *J. Geophys. Res.*, *104*, 30445-30462, 1999.
- Swap, R., M. Garstang, S. A. Macko, P. D. Tyson, W. Maenhaut, P. Artaxo, P. Kallberg, R. Talbot, The long-range transport of southern African aerosols to the tropical South Atlantic, *J. Geophys. Res.*, *101*, 23777-23791, 1996.
- Talbot, R. W., J. D. Bradshaw, S. T. Sandholm, S. Smyth, D. R. Blake, N. J. Blake, G. W. Sachse, J. E. Collins, Jr., B. G. Heikes, B. E. Anderson, G. L. Gregory, H. B. Singh, B. L. Lefer, and A. S. Bachmeier, Chemical characteristics of continental outflow over the tropical South Atlantic Ocean from Brazil and Africa, *J. Geophys. Res.*, *101*, 24187-24202, 1996.
- Talbot, R. W., J. E. Dibb, E. M. Scheuer, D. R. Blake, N. J. Blake, G. L. Gregory, G. W. Sachse, J. D. Bradshaw, S. T. Sandholm, and H. B. Singh, Influence of biomass combustion emissions on the distribution of acidic trace gases over the southern Pacific basin during austral springtime, *J. Geophys. Res.*, *104*, 5623-5634, 1999.
- Vay, S. A., B. E. Anderson, T. J. Conway, G. W. Sachse, J. E. Collins Jr., D. R. Blake, and D. J. Westberg, Airborne observations of the tropospheric CO₂ distribution and its controlling factors over the South Pacific basin, *J. Geophys. Res.*, *104*, 5663-5676, 1999.

BIOGRAPHICAL SKETCH

Danielle Morse was born in Danvers, Mass. on May 4, 1980. She grew up in Washington D.C. with her parents and two brothers. An early affinity for maps, science and space gradually led her to a deep interest in the atmospheric sciences. She graduated from the National Cathedral School for Girls in June 1998 and entered the Massachusetts Institute of Technology in the fall of that year.

While at MIT, Danielle was an undergraduate research assistant to Prof. Reginald Newell and worked on data from three NASA-GTE missions: SONEX, PEM-Tropics B, and TRACE-Pacific. In her spare time, she was a member of the varsity fencing team and the MIT Guild of Bellringers. Danielle graduated from MIT in June 2002 with an S.B. in Earth, Atmospheric and Planetary Sciences and a minor in Physics. She then moved to Tallahassee, FL to pursue a master's degree in Meteorology at the Florida State University. While at FSU, she has been a member of Dr. Henry Fuelberg's lab and been involved with three more NASA-GTE missions: TRACE-A, PEM-Tropics A and INTEX-A.